Optics Letters

Hybrid fiber–solid-state laser with 3D-printed intracavity lenses

Simon Angstenberger,* Pavel Ruchka, Mario Hentschel, Tobias Steinle, and Harald Giessen

4th Physics Institute and Stuttgart Research Center of Photonic Engineering, University of Stuttgart, Pfaffenwaldring 57, 70569 Stuttgart, Germany
**simon.angstenberger@pi4.uni-stuttgart.de*

Received 19 September 2023; revised 27 October 2023; accepted 4 November 2023; posted 21 November 2023; published 13 December 2023

Microscale 3D-printing has revolutionized micro-optical applications ranging from endoscopy, imaging, to quantum technologies. In all these applications, miniaturization is key, and in combination with the nearly unlimited design space, it is opening novel, to the best of our knowledge, avenues. Here, we push the limits of miniaturization and durability by realizing the first fiber laser system with intra-cavity on-fiber 3D-printed optics. We demonstrate stable laser operation at over 20 mW output power at 1063.4 nm with a full width half maximum (FWHM) bandwidth of 0.11 nm and a maximum output power of 37 mW. Furthermore, we investigate the power stability and degradation of 3D-printed optics at Watt power levels. The intriguing possibilities afforded by free-form microscale 3D-printed optics allow us to combine the gain in a solid-state crystal with fiber guidance in a hybrid laser concept. Therefore, our novel ansatz enables the compact integration of a bulk active media in fiber platforms at substantial power levels.

https://doi.org/10.1364/OL.504940

Introduction. The downsizing of optical components has become a necessity in many applications. With the increasing demand for portability and miniaturization of devices, the size of optical to functionality and performance are maintained. This trend has led to the development of micro-optics [1–4] and nanophotonics, which deal with the fabrication and characterization of optical components at reduced sizes [5,6]. Small-scale components provide wider application ranges and reduce the overall cost [7]. Therefore, the downsizing of optical components and even lasers has become a vital aspect of modern optics and photonics research [8–13]. Thus, a system is desirable that extends integrated photonic devices [14,15] toward the incorporation of bulk solid-state laser media [16,17].

The advent of 3D-printing of micro-optics by direct laser writing has enabled miniature optical elements with ever-increasing complexity [12,18,19]. These micro-optical elements are typically designed for low-power applications in endoscopy [20,21] or in quantum technologies such as atomic trapping [22]. While prior investigations [23,24] have touched upon the functionality of 3D-printed optics under Watt power levels, our study distinguishes itself by successful integration of 3D-printed aspherical lenses within a practical device. This underscores their real-world applicability, despite recent findings from Klein *et al.* of damages within 3D-printed structures upon laser light exposure [25]. As it is possible to implement these microscale optics for complex beam shaping and integrated optics [26,27], they present themselves as an ideal candidate for several laser applications.

In this paper, we combine the gain in a Nd:YVO_4 solid-state laser crystal and light guidance in fibers for all other optical components. We use 3D-printed micro-optics in the form of on-fiber lenses for fiber coupling. This reduces the footprint of the coupling stage. The laser system exhibits stable output power at over 20 mW with only 0.3% root mean square (rms) fluctuations and a maximum output power of 37.4 mW. This sets the framework for almost-all-fiber amplifier chains with bulk gain crystals or even power scaling of fiber oscillators [28–30].

In our implementation of the hybrid laser system, we apply pump powers of over 2 W. The printed lens does not affect pump power stability and shows no visible degradation even after several hours of laser operation. This expands the application range of these optics to the Watt power regime. In turn, we demonstrate the potential of complex micro-optics fabricated with direct laser lithography.

Setup. The laser cavity is established between the left end facet of the laser crystal and a partially reflective fiber Bragg grating (FBG) as shown in Fig. 1(a). The crystal is a 3 mm × 3 mm × 5 mm Nd:YVO_4 crystal with 0.5% doping level, pumped by a 808 nm diode. The left end facet of the crystal acts as a pump mirror through a highly reflective coating at the lasing wavelength of 1064 nm while being transmissive for the pump light. The other end facet is anti-reflection coated for both the pump and signal wavelength. The pump diode delivers up to 5 W output power through a multi-mode FG105LCA fiber (105 µm core diameter). The cavity lasing light is fiber-guided in single-mode polarization-maintaining PM980XP fiber. The FBG extracts 30% of the laser light upon reflection. The beams of the 3D-printed optics are overlapped without the crystal in

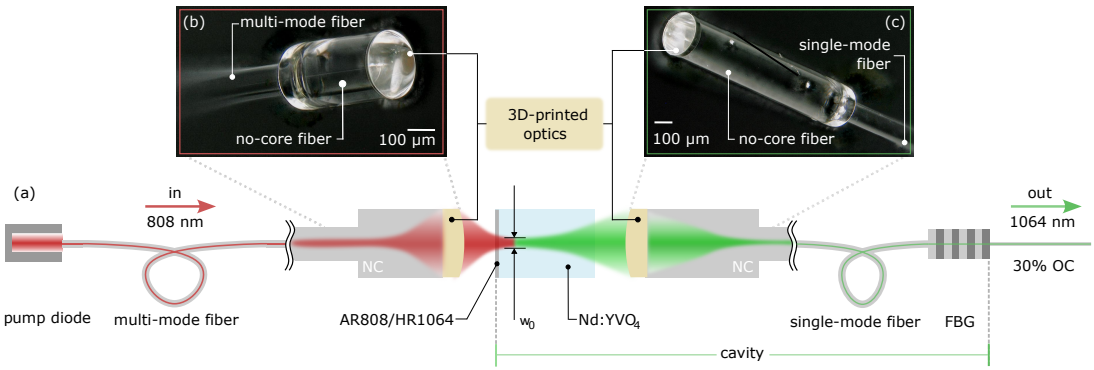

Fig. 1. Schematic of the laser design implementing 3D-printed lenses for fiber coupling. (a) An 808 nm laser diode is used to pump a Nd:YVO_4 crystal. The laser cavity is established between the 1064 nm high-reflection coated end facet of the crystal (HR, marked in silver) and a partially reflective fiber Bragg grating (FBG) which acts as an output coupler (OC) with a ratio of 30%. Pump diode input (red) and laser output (green) are fully fiber-guided in the multi-mode FG105LCA and the single-mode PM980XP fiber, respectively. NC: no-core fiber piece, spliced onto the fibers with cores, for beam expansion. (b) Microscope image of the 3D-printed lens on top of a no-core fiber piece at 200× magnification for pump beam focusing. (c) Microscope image of the intra-cavity 3D-printed lens, recorded with 200× magnification.

place, using two three-axis translation stages. Subsequently, the crystal on a rotation mount is placed between the fibers. Back-coupling into the cavity fiber is maximized using an alignment laser. The fibers are then glued into the crystal mount for added stability.

Both laser beam and the pump beam are focused toward the crystal with 3D-printed lenses which are shown in Fig. 1(b), (c). No-core fibers (FG250LA) with 250 µm diameter and lengths of 470 µm and 1370 µm spliced onto the respective fibers are used for beam expansion to utilize the full aperture of the lens commensurate with the fiber numerical apertures.

A detailed view of the beam expansion is given in the upper part of Fig. 2. The upper left panel illustrates the pump focusing scheme. The pump lens focuses the light on the left crystal end facet with a short working distance of approximately 357 µm limited by the beam quality given by the multimode fiber. Ruchka *et al.* [22] have previously shown a detailed description of the on-fiber 3D-printing process.

The upper right panel of Fig. 2 shows the beam path for the cavity light. The beam is focused toward the end facet of the crystal, therefore making a working distance in the mm range necessary. The single-mode nature of the PM980XP fiber requires a longer piece of no-core fiber. A housing around the setup with a footprint of 40 cm × 25 cm is set up for laser safety. The footprint of lens-crystal-lens free space part (*cf.* exploded view in Fig. 1) is only 5 cm x 5 cm.

Results and discussion. Both pump and cavity light are focused toward the left end facet of the crystal that defines one end of the cavity. In contrast to a simple cleave, the polymer lens allows focusing of the beam at a specific distance. Thus, the lower section in Fig. 2 plots the beam profiles in the focal spot for pump (left) and signal (right).

The pump beam profile yields a speckled beam profile, which can be attributed to the limited beam quality stemming from the multi-mode FG105LCA fiber. The signal beam profile in (d) exhibits an asymmetry, but the mode is cleaner due to single-mode guidance in the PM980XP fiber. Designed FWHM for pump and signal were 41 µm and 60 µm whereas the measured values are 67/64 µm and 23/27 µm, respectively. In iterative steps, the efficiency could benefit from adapted lens designs to achieve better matching beam profiles.

As the lasing of the setup requires pump powers in the Watt regime passing through the plastic lenses, we evaluated the power stability of the pump unit. The power stability of the pump beam was recorded as depicted in Fig. 3(a). After a cleaved end facet of the pump fiber, an average power of 2.53 W with a fluctuation of 0.2% rms was measured. Subsequently, the combination of the FG105LCA-NC250-pump lens was spliced to that cleave, and the power was once more measured for 1 h.

As the fluctuation is 0.3% rms at 2.06 W, we conclude that the 3D-printed lens has no significant effect on the stability of the pump light delivery, even though the maximum intensity in the beam center exceeds 8.67 kW cm^{-2} at 2.06 W. This was verified by an optical investigation of the lens arrangements (b) before use and (c) after use by means of scanning electron microscopy (SEM). Panel (c), recorded after several (>5 h) of laser operation at powers >1 W, shows no visible degradation. The small features are dust/dirt particles.

The laser characteristics of the overall system are presented in Fig. 4. A maximum laser output power of 37.2 mW at an outcoupling ratio of 30% only limited by the failure of the fiber Bragg grating at intracavity powers >100 mW is measured (b). The corresponding spectra (*cf.* colored dots in the slope) are plotted above the slope in Panel (a). The FBG shifts the central wavelength to 1063.4 nm at 0.11 nm FWHM bandwidth with a stable spectral shape ranging over the entire output power range. A slight offset from the nominal maximum gain of Nd:YVO_4 due to the central wavelength of the FBG affects maximum possible efficiency of the setup. After some thermalization effects, the initial output power of 24.1 mW at 1.8 W pump power settles to 20.57 mW power and fluctuates only by 0.3% rms around the mean for an hour of recording time. This corresponds to a maximum intracavity intensity of 590 W cm^{-2} in the center of the beam at the lens. We attribute these fluctuations mainly to pump power fluctuations, *cf.* Fig. 3. The inset displays the rms value and the average value as well. The slope efficiency of 3% stems from a 16% back-coupling efficiency at the signal lens, with 30% OC ratio this results in a Q factor of 0.15. This efficiency could be increased by improved mode matching, where one might consider thermal lensing in improved aberration pre-correction steps. Thermal load in the FBG limits the maximum output power of the setup. The FBG was chosen

for its in-stock availability. The implementation of a high-power FBG, mounted on a thermal heat sink, could aid to overcome this limitation. This would help to explore the power scalability limit of the printed optics inside the cavity, which do not yet limit the maximum achievable output power.

Conclusion. We have demonstrated the successful integration of microscale 3D-printed optics in a laser system at up to 37.4 mW output power and over 2 W pump power. This combination of the laser gain in a solid-state crystal and the all-fiber guidance for all other components is a promising avenue for active optical component downsizing. Accordingly, properties of fiber lasers such as wavelength range can be extended through the variety of physical properties offered by bulk media.

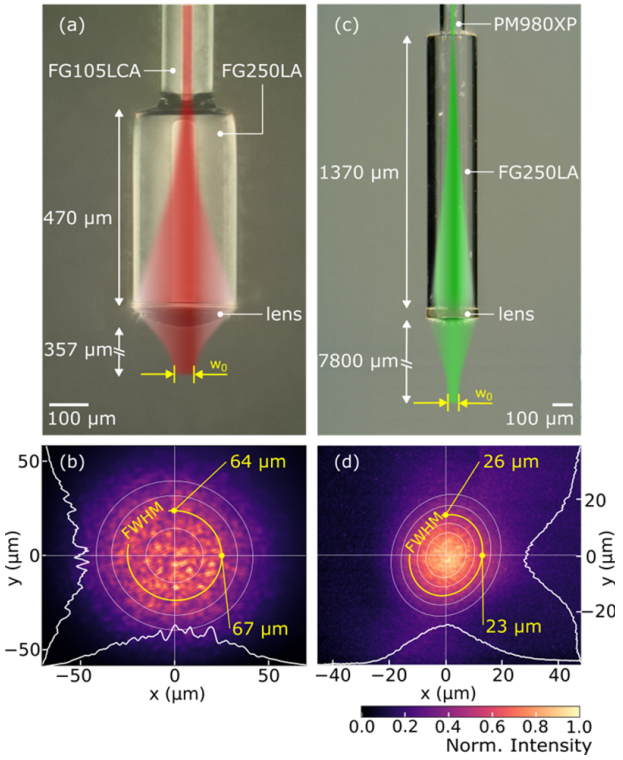

Fig. 2. Lens designs and beam profiles at the focal spot. Image (a), captured with an optical microscope at 100× magnification, schematically illustrates the beam expansion of the 808 nm pump light (red) from the diode-connected FG105LCA multi-mode fiber in a 470 µm long piece of FG250LA no-core fiber with 250 µm diameter. The lens focuses the beam toward a focal spot w_0 at 357 µm working distance (not to scale) with the corresponding beam profile indicated in (b). It exhibits an approximately symmetric profile, fitted with a Gaussian as indicated by the circular-shaped white contour lines. The Gaussian FWHM is marked in yellow with $FWHM_x = 67$ µm and $FWHM_y = 64$ µm, respectively. The white curves at the x and y axis show the sum of the central 20 pixel lines in the respective dimensions. Panel (c), captured with an optical microscope at 60× magnification, displays the propagation of the cavity laser light beam (green) similar to (a). The beam at 1064 nm wavelength is fiber-coupled to a PM980XP fiber by means of a 1370 µm long piece of FG250LA no-core fiber with 250 µm diameter. (d) Beam profile of the signal light at the focal point, imaged at 60× magnification, plotted in a similar manner as (b). The Gaussian FWHM (yellow) is smaller with $FWHM_x = 23$ µm and $FWHM_y = 26$ µm, respectively.

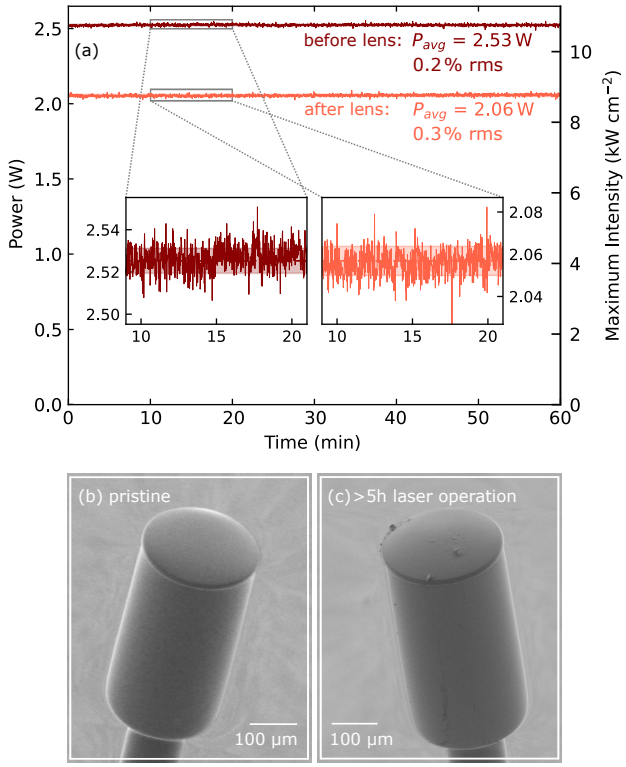

Fig. 3. Power stability and visual inspection of the printed pump lens before and after use. (a) Power stability measurement of the pump light taken before (dark red) and after (bright red) the light passed through the printed lens. Before the lens, the power exhibits 0.2% rms fluctuation around a nominal value of 2.53 W. The stability after the lens was measured at an average power of 2.06 W, corresponding to 8.67 kW cm^{-2} intensity in the center of the lens. Panel (b) displays an SEM image of the lens before use at 80× magnification, while panel (c) shows an SEM image of the lens at 110× magnification after over 5 h exposure to pump light powers of over 1 W. In agreement with optical observations, no visible damage is observed in the lens despite continuous use, apart from dust particles.

Overall, the presented performance of 3D-printed optics inside a lasing cavity provides the base for subsequent investigation at substantial power levels, also addressing long-term stability on a larger time scale. not limited to laser applications. Established fields that already use complex laser lithography-based free-form optics [19] could make use of the watt power handling capabilities shown in this Letter [20,21,24].

Funding. Bundesministerium für Bildung und Forschung (KMU MIR-SWEEP); European Research Council (PoC 3DPRINTEDOPTICS); Carl-Zeiss-Stiftung; Deutsche Forschungsgemeinschaft (GRK2642); Center for Integrated Quantum Science and Technology (IQST); Baden-Württemberg Stiftung.

Acknowledgments. S.A. would like to thank Moritz Floess for helpful discussion regarding data evaluation.

Disclosures. The authors declare no conflicts of interest.

Data availability. Data underlying the results presented in this paper are not publicly available at this time but may be obtained from the authors upon reasonable request.

Supplemental document. See Supplement 1 for supporting content.

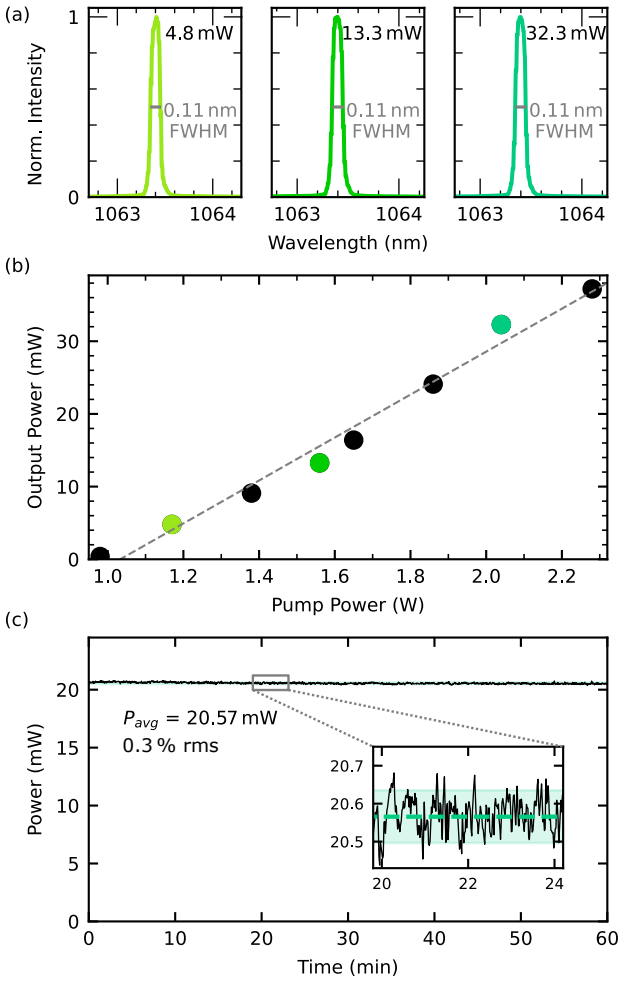

Fig. 4. Characterization of the hybrid fiber–solid-state laser. Panel (a) displays the spectra at increasing output power levels marked with the respective color in (b). The spectra confirm a narrow linewidth centered at 1063.4 nm with 0.11 nm FWHM and no visible alteration of the spectral shape across the entire output power range. Panel (b) indicates the power versus pump slope with a slope efficiency of 3.0%. The maximum output power is 38.9 mW. Panel (c) plots the stability at 20.57 mW. The inset depicts the rms-area shaded in mint around the average value (dashed line) for around four minutes of the measurement.

REFERENCES

1. M. Thiel, J. Fischer, G. von Freymann, *et al.*, Appl. Phys. Lett. **97**, 221102 (2010).
2. M. Malinauskas, P. Danilevičius, and S. Juodkazis, Opt. Express **19**, 5602 (2011).
3. T. Gissibl, S. Thiele, A. Herkommer, *et al.*, Nat. Photonics **10**, 554 (2016).
4. T. Gissibl, S. Thiele, A. Herkommer, *et al.*, Nat. Commun. **7**, 11763 (2016).
5. W. Liang, V. S. Ilchenko, D. Eliyahu, *et al.*, Nat. Commun. **6**, 7371 (2015).
6. M. Yuan, X. Han, H. Xiao, *et al.*, Opt. Lett. **48**, 171 (2023).
7. Z. Ma, J. Sun, S. Zhou, *et al.*, Opt. Lett. **48**, 139 (2023).
8. D. Perevoznik, A. Tajalli, D. Zuber, *et al.*, J. Lightwave Technol. **39**, 4390 (2021).
9. Y. Feng, T. P. Lamour, H. Ostapenko, *et al.*, Opt. Lett. **46**, 5429 (2021).
10. H. Ostapenko, Y. Feng, T. Lamour, *et al.*, Opt. Express **31**, 3249 (2023).
11. E. Türkyilmaz, J. Lohbreier, C. Günther, *et al.*, Opt. Eng. **55**, 066126 (2016).
12. L. Yang, F. Mayer, U. H. F. Bunz, *et al.*, Light: Adv. Manuf. **2**, 17 (2021).
13. Y. Wang, J. A. Holguín-Lerma, M. Vezzoli, *et al.*, Nat. Photonics **17**, 338 (2023).
14. L. Orsila, J. Sand, M. Närhi, *et al.*, Optica **2**, 757 (2015).
15. O. Melchert, C. Brée, A. Tajalli, *et al.*, Commun. Phys. **3**, 146 (2020).
16. F. Schepers, T. Bexter, T. Hellwig, *et al.*, Appl. Phys. B **125**, 75 (2019).
17. C. A. A. Franken, A. van Rees, L. V. Winkler, *et al.*, Opt. Lett. **46**, 4904 (2021).
18. C. A. Richards, C. R. Ocier, D. Xie, *et al.*, Nat. Commun. **14**, 3119 (2023).
19. L. Siegle, S. Ristok, and H. Giessen, Opt. Express **31**, 4179 (2023).
20. J. Li, S. Thiele, R. W. Kirk, *et al.*, Small **18**, e2107032 (2022).
21. S. Sivankutty, A. Bertoncini, V. Tsvirkun, *et al.*, Opt. Lett. **46**, 4968 (2021).
22. P. Ruchka, S. Hammer, M. Rockenhäuser, *et al.*, Quantum Sci. Technol. **7**, 045011 (2022).
23. I. V. A. K. Reddy, A. Bertoncini, C. Liberale, *et al.*, Optica **9**, 645 (2022).
24. S. Singer, Y. Xu, S. T. Skacel, *et al.*, Opt. Express **30**, 46564 (2022).
25. S. Klein, P. Ruchka, T. Klumpp, *et al.*, Opt. Mater. Express **13**, 3653 (2023).
26. V. Purlys, L. Maigyte, D. Gailevičius, *et al.*, Opt. Lett. **39**, 929 (2014).
27. M. Schumann, T. Bückmann, N. Gruhler, *et al.*, Light: Sci. Appl. **3**, e175 (2014).
28. H. Zimer, M. Kozak, A. Liem, *et al.*, Proc. SPIE **7914**, 791414 (2011).
29. Y. Xiao, F. Brunet, M. Kanskar, *et al.*, Opt. Express **20**, 3296 (2012).
30. M. Prossotowicz, A. Heimes, D. Flamm, *et al.*, Opt. Lett. **45**, 6728 (2020).